Biosensors and Bioelectronics 26 (2011) 4491–4496

Contents lists available at ScienceDirect

Biosensors and Bioelectronics

journal homepage: www.elsevier.com/locate/bios

Self-assembled graphene platelet–glucose oxidase nanostructures for glucose biosensing

Sen Liu [a], Jingqi Tian [a,b], Lei Wang [a], Yonglan Luo [a], Wenbo Lu [a], Xuping Sun [a,*]

[a] State Key Lab of Electroanalytical Chemistry, Changchun Institute of Applied Chemistry, Chinese Academy of Sciences, Changchun 130022, Jilin, PR China
[b] Graduate School of the Chinese Academy of Sciences, Beijing 100039, China

ARTICLE INFO

Article history:
Received 4 March 2011
Received in revised form 19 April 2011
Accepted 4 May 2011
Available online 11 May 2011

Keywords:
Self-assembly
Graphene platelets
Glucose oxidase
Nanostructure
Biosensor

ABSTRACT

Graphene platelet–glucose oxidase (GP–GOD) nanostructures have been prepared through self-assembly of GOD and chitosan (CS) functionalized GPs by electrostatic attraction in aqueous solution. The stable aqueous dispersion of GPs was prepared by chemical reduction of graphene oxide with the use of CS as a reducing and stabilizing agent. UV–vis spectroscopy, X-ray diffraction, transmission electron microscopy, scanning electron microscopy and X-ray photoelectron spectroscopy were used to characterize the resulting GPs and GP–GOD nanostructures. Furthermore, a glucose biosensor was constructed by deposition of the resultant GP–GOD on the surface of glassy carbon electrode. It was found that the resulting biosensor exhibits good response to glucose. The linear detection range is estimated to be from 2 to 22 mM (r = 0.9987), and the detection limit is estimated to be 20 μM at a signal-to-noise ratio of 3.

1. Introduction

Since the discovery by Geim and Novoselov (2007), graphene, a flat monolayer of sp^2-bonded carbon atoms tightly packed into a two-dimensional (2D) honeycomb lattice, and characterized as "the thinnest material in our universe" (Novoselov et al., 2004; Allen et al., 2010; Rao et al., 2009), has received considerable attention due to its high surface area (~2600 m^2/g), high chemical stability, and unique electronic, mechanical properties, which ensure its potential applications in nanoelectronics, hybrid, Li ion batteries, and sensors (Dikin et al., 2007; Stankovich et al., 2006; Yoo et al., 2008; Zhang et al., 2005; Zhou et al., 2009a; Kang et al., 2009) Particularlly, recent research has shown that graphene is a promising candidate for biosensing nanomaterials, opening the door for the construction of biosensors using graphene-based materials (Liu et al., 2010a,b,c; Shao et al., 2010). Although there are a large amount of bi-layer and multi-layer graphenes formed by chemical reduction of graphene oxide (GO), a recent review indicates that these materials also exhibit excellent catalytic performance for biosening applications, compared with single layer graphene (Pumera et al., 2010). Thence, the use of chemical reduced GO (rGO) for the construction of biosensors has received much attention. Up to now, numerous approaches have been successfully developed to fabricate graphene-based biosensors based on graphene-based materials (Liu et al., 2010a,b,c; Lu et al., 2008, 2010; Shan et al., 2009, 2010; Wang et al., 2009b, 2010a; Wu et al., 2009, 2010; Xu et al., 2010; Yang et al., 2010a; Zeng et al., 2010a; Zhou et al., 2010a,b). For example, enzyme-based biosensors can be constructed by immobilization of enzyme into graphene films on the electrode surface with the aid of chitosan (CS), nafion, as well as ionic liquid (Liu et al., 2010a,b,c; Shan et al., 2009; Wang et al., 2009b, 2010a; Wu et al., 2010; Xu et al., 2010; Yang et al., 2010a; Zeng et al., 2010a). To further improve their catalytic performance, noble metal nanoparticles are also involved to fabricate enzyme-graphene films on the surface of electrode for biosensing (Lu et al., 2008; Shan et al., 2010; Wu et al., 2009; Zhou et al., 2010a,b). It is well-known that graphene-based materials play an important role in improving the catalytic performance for biosnesing because the unique properties of graphene such as high surface area, excellent conductivity and small band gap result in high loading of enzyme moleculars and improving electrons transfer rate from biomolecules to electrode (Kang et al., 2009). However, all the above graphene-based hybrids are prepared on the surface of electrode, which limits their wide applications in energy storage, photovoltaic device, drug delivery, etc.

Recent progress in synthesis of graphene-based hybrid by a self-assembly route has promoted extensive exploration of graphene-based biosensors (Choi et al., 2010; Patil et al., 2009; Zeng et al., 2010b). For example, Patil et al. (2009) have prepared graphene and single stranded-DNA (ss-DNA) hybrid by an aqueous co-assembly route, opening the door for the construction of graphene-based hybrid for biosensing and biotechnology. More

* Corresponding author. Tel.: +86 431 85262065; fax: +86 431 85262065.
E-mail address: sunxp@ciac.jl.cn (X. Sun).

0956-5663/$ – see front matter © 2011 Elsevier B.V. All rights reserved.
doi:10.1016/j.bios.2011.05.008

recently, Zeng et al. (2010b) have reported that graphene-enzyme hierarchical nanostructures are fabricated by self-assembly of negatively charged sodium dodecyl benzene sulphonate (SDBS) stabilized graphene with positively charged horseradish peroxidase (HRP) through electrostatic interactions. However, this synthetic route has a obvious disadvantage of the use of hydrazine, which is highly poisonous and potentially exposive chemicals (Li et al., 2008). Accordingly, the exploration of environmental friendly route to self-assembly of graphene-enzyme nanostructures for biosensing applications is highly desired.

CS has attracted significant interest because of its good biocompatibility, biodegradability, and much multiple functional groups (Huang et al., 2004; Potara et al., 2009). It has been demonstrated that CS is a good stabilizing agent for both GO and graphene (Fang et al., 2010; Wang et al., 2010b; Yang et al., 2010b; Zhou et al., 2010c). To the best of our knowledge, however, the use of CS as a reducing agent for GO has not been addressed so far. In the present study, we report on our recent finding that stable dispersion of graphene platelets (GPs) can be obtained by chemical reduction of GO with the use of CS as a reducing and stabilizing agent, providing us a green route to the easy preparation of GPs. We further domenstrate that the GP–enzyme nanostructures can be formed by a self-assembly route, where positively charged CS not only prevent GP from aggregation, but also drive the assembly of negatively charged glucose oxidase (GOD) and GPs into nanostructures. Furthermore, a glucose biosensor was constructed by deposition of the resultant GP–GOD on the surface of glassy carbon electrode (GCE). It was found that the resulting biosensor exhibits good response to glucose.

2. Experimental

2.1. Materials

CS, H_2O_2 (30 wt%) and graphite powder were purchased from Aladin Ltd. (Shanghai, China). GOD was purchased from Aldrich Chemical Comp. H_2SO_4, $NaNO_3$, glucose, Na_2HPO_4, NaH_2PO_4, $KMnO_4$, $K_3Fe(CN)_6$, and KCl were purchased from Beijing Chemical Comp. All chemicals were used as received without further purification. The water used throughout all experiments was purified through a Millipore system. Phosphate buffer saline (PBS) was prepared by mixing stock solutions of NaH_2PO_4 and Na_2HPO_4 and a fresh solution of H_2O_2 was prepared daily.

2.2. Preparation of GO

GO was prepared from natural graphite powder through a modified Hummers method (Hummers and Offeman, 1958). In a typical synthesis, 1 g of graphite was added into 23 mL of 98% H_2SO_4, followed by stirring at room temperature over a period of 24 h. After that, 100 mg of $NaNO_3$ was introduced into the mixture and stirred for 30 min. Subsequently, the mixture was kept below 5 °C by ice bath, and 3 g of $KMnO_4$ was slowly added into the mixture. After heating to 35–40 °C, the mixture was stirred for another 30 min. After that, 46 mL of water was added into above mixture during a period of 25 min. Finally, 140 mL of water and 10 mL of H_2O_2 were added into the mixture to stop the reaction. After the unexploited graphite in the resulting mixture was removed by centrifugation, as-synthesized GO was dispersed into individual sheets in distilled water at a concentration of 0.5 mg/mL with the aid of ultrasound for further use.

2.3. Preparation of GPs

In a typical synthesis, 1 mL of aqueous GO dispersion was added into 2 mL of H_2O, followed by addition of 1 mL of CS solution (0.5 M). After stirring at room temperature for 30 min, the mixture was heated to 90 °C over a period of 2 h. Finally, the black dispersion of GP stabilized by CS at a concentration of 0.125 mg/mL was obtained.

2.4. Preparation of GP–GOD nanostructures

In a typical synthesis, 10 μL of GOD solution (10 mg/mL) was added into 20 μL of GP dispersion, followed by ultrasonic treatment 10 min. Then the mixture was kept at 4 °C for 12 h. After that, a large amount solid product was formed. The GP–GOD nanostructures were obtained after removal of the water. The resulting GP–GOD nanostructures were then dispersed in 10 μL of water and were stored at 4 °C for further use.

2.5. Fabrication of the GP–GOD nanostructures modified GCE

The modified electrodes were prepared by a simple casting method. Prior to the surface coating, the GCE was polished with 1.0 and 0.3 μm alumina powder, respectively, and rinsed with doubly distilled water, followed by sonication in ethanol solution and doubly distilled water successively. Then, the electrode was allowed to dry in a stream of nitrogen. For the cyclic voltammetry experiment, 2 μL of the GP–GOD nanostructures dispersion was dropped on the clean surface of GCE, and dried at 4 °C. The GOD-modified GCE (GOD/GCE), CS-modified GCE (CS/GCE) and GP-modified GCE (GP/GCE) were prepared by dropping 2 μL of 10 mg/mL GOD containing 1 mL of 0.5 M CS, 2 μL of 0.5 M CS and 2 μL of GP dispersion, respectively.

2.6. Characterization

UV–vis spectra were collected on a UV5800 Spectrophotometer. Transmission electron microscopy (TEM) measurement was made on a HITACHI H-8100 EM (Hitachi, Tokyo, Japan) with an accelerating voltage of 200 kV. Scanning electron microscopy (SEM) measurements were made on a XL30 ESEM FEG scanning electron microscope at an accelerating voltage of 20 kV. Powder X-ray diffraction (XRD) data were recorded on a Rigaku D/MAX 2550 diffractometer with Cu Kα radiation (λ = 1.5418 Å). X-ray photoelectron spectroscopy (XPS) analysis was measured on an ESCALABMK X-ray photoelectron spectrometer. Electrochemical measurements are performed with a CHI 660D electrochemical analyzer (CH Instruments, Inc., Shanghai). A conventional three-electrode cell was used, including a GCE (geometric area = 0.07 cm^2) as the working electrode, a Ag/AgCl (saturated KCl) electrode as the reference electrode, and platinum foil as the counter electrode. The potentials are measured with a Ag/AgCl electrode as the reference electrode. All the experiments were carried out at ambient temperature.

3. Results and discussion

The reduction kinetics of GO was first studied by time-dependent UV–vis spectra of the GO–CS mixture during the heat treatment process, as shown in Fig. 1a. Notably, GO exhibits strong bands centred at 230 and 300 nm, corresponding to $\pi \rightarrow \pi^*$ transitions of aromatic C=C band and $n \rightarrow \pi^*$ transitions of C=O band in GO, respectively (Zhou et al., 2009a,b). It is clearly seen that the absorption peak gradually red-shifts from 230 to 260 nm and the absorbance in the whole spectral region increases with the elapsed time. Such observations suggest that the electronic conjugation within the GO is restored upon the heat treatment (Guo et al., 2010). Fig. 1a inset shows the photographs of GO–CS mixture before (left) and after (right) the heat treatment process, revealing a distinct color change from pale-yellow to black. Such observation provides another piece of evidence to support the formation

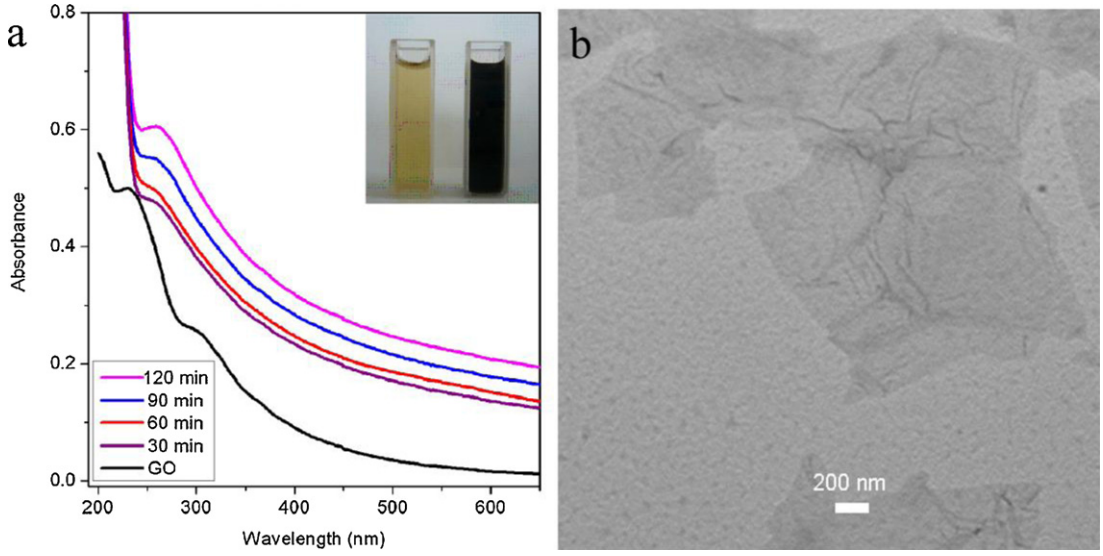

Fig. 1. (a) Time-dependent UV–vis spectra of GO–CS mixture during the heat treatment process. Inset: photographs of the aqueous dispersions of GO (left) and GP (right) and (b) TEM image of GP thus formed.

of GP (Zhu et al., 2010). It should be noted that no change was observed for the GO dispersion if it is heated in the absence of CS, indicating that the formation of GP can be attributed to the chemical reduction of GO by CS. It is also worthwhile mentioning that the dispersion thus formed can be very stable for several months without the observation of any floating or precipitated particles, which can be attributed to the good stabilizing ability of CS for GP (Fang et al., 2010). Fig. 1b shows typical TEM image of the resulting GP, indicating the formation of isolated nanosheets.

Fig. S1 shows the XRD patterns of graphite powder, GO, and resulting GP. It is found that graphite powder (Fig. S1a) shows a sharp (0 0 2) peak at 26.4° with a typical inter-spacing of 3.35 Å (Li et al., 2009; Nethravathi and Rajamathi, 2008). In contrast, GO exhibits a strong peak at 10.02° corresponding to the (0 0 2) interplanar spacing of 8.2 Å (Fig. S1b), suggesting graphite has been successfully oxidized by Hummers method (Pham et al., 2010). It is observed that the corresponding peak disappears after the heat treatment process (Fig. S1c), confirming the reduction of GO (Zhang et al., 2010).

Fig. S2 shows the XPS spectra of GO and GP. It is well known that the bands centred at 284.8 and 531.0 eV are associated with C1s and O1s, respectively (Li et al., 2009). It is interesting to have found that O1s intensity of GP significantly decreased compared with that of GO, suggesting the loss of oxygen in GO (Zhang et al., 2010). It is also found that another band at 400 eV is observed, which is attributed to the N element of CS, indicating the presence of CS (Wang et al., 2009a). Fig. 2 shows the C1s XPS spectra of GO and GP, respectively. The C1s spectra of GO and GP could be deconvoluted into four peaks at 284.5, 285.6, 286.6, and 288.4 eV, which are associated with C–C, C–OH, C(epoxy/alkoxy), and C═O groups, respectively (Fan et al., 2008). It is obviously seen that the peak intensity of C–O and C═O in strong in GO (Fig. 2a); in contrast, after heat treatment process, the peak intensity of C–O and C═O in GPs (Fig. 2b) tremendously reduced, and the content of C–C correspondingly increases dramatically (Park et al., 2008). In addition, it is also seen that a new peak at 286 eV is observed, further confirming the presence of CS (Yang et al., 2010b). All these observations suggest that the most oxygen-containing functional groups are successfully removed after heat treatment process.

Because CS is positively charged due to the protonation of its $-NH_2$ group, it is expected that the resulting GPs can be easily assembled with negatively charged enzyme GOD through electrostatic attraction interactions. Herein, we construct GP–GOD nanostructures by self-assembly of CS-stabilized GP and GOD. Fig. 3a shows the SEM images of GP–GOD nanostructures thus formed. It is obviously seen that the sample comprises multiple sheets of the GPs. In addition, the GP–GOD exhibits many cracks

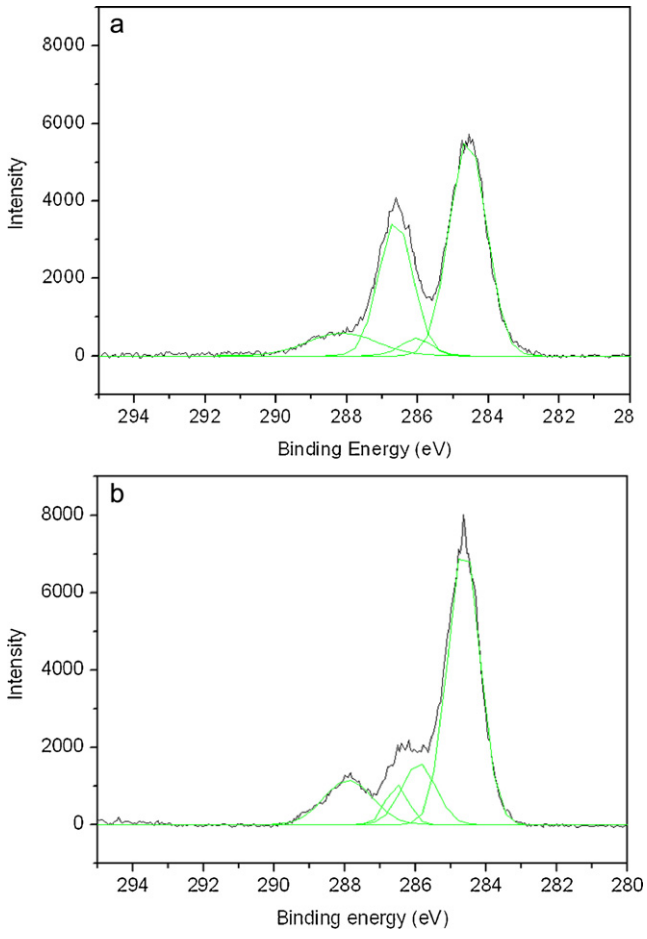

Fig. 2. C1s XPS spectra of GO (a) and GP (b).

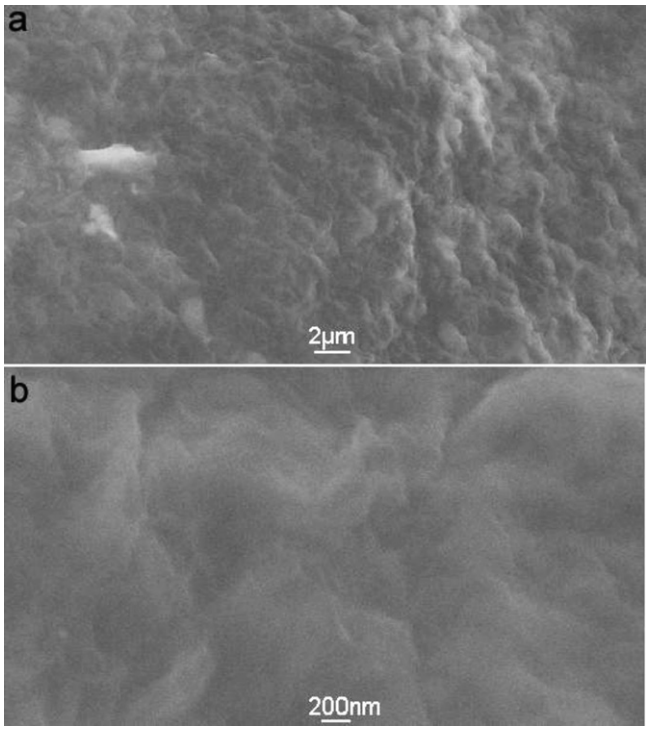

Fig. 3. (a) Low and (b) high magnification SEM image of GP–GOD nanostructures.

and high surface roughness, indicating that the novel composites could increase the electroactive surface area of the modified electrodes. The close-up view further confirms the self-assembly of GP and GOD nanocomposites (Fig. 3b). This observation confirms the formation of GP–GOD nanostructures by self-assembly route. Fig. 4 presents a scheme (not to scale) to illustrate the formation of GP from GO with the use of CS as a reducing and stabilizing agent and the subsequent preparation of GP–GOD nanostructures by a self-assmbly route. It should be noted that the formation of graphene from GO can be attributed to the direct redox between the $-NH_2$ group of CS and GO, because there is no other reducing agent in this system. Indeed, CS has been used as a reducing agent for preparation of metal nanoparticles (Huang et al., 2004; Wei et al., 2009). It also should be mentioned that the resulting dispersion of GPs is very stable, suggesting CS serves as a good stabilizing agent for GP. Furthermore, CS contains large amount of 6-membered rings of carbon, and a hydrophilic biopolymer with –OH and $-NH_2$ in each unit (Huang et al., 2004). It is expected that residual oxygen-containing groups and the GPs have the opportunity to capture –OH and $-NH_2$ groups of CS by zwitterionic interaction and hydrogen bonding, by which the CS could be non-covalently bonded to the GPs and endowed with dispersibility in water (Fang et al., 2010). On the other hand, the positively charged CS can be assembled with negatively charged enzyme GOD by electrostatic attraction interactions. Thus, GP–GOD nanostructures were successfully prepared by the self-assemble route.

Fig. S3 shows the cyclic voltammograms (CVs) of bare GCE, CS/GCE and GP/GCE in 1.0 mM KCl solution containing 2.0 mM $K_3Fe(CN)_6$. It is seen that relative week redox peaks were observed on CS/GCE, indicating the slow electrons transfer kinetics of $Fe(CN)_6^{4-/3-}$ due to the presence of CS layer on the electrode (Kang et al., 2009). In contrast, a pair of redox peaks was obtained on GP/GCE, although the peak current obtained was smaller than that of bare GCE at the same condition, indicating that GP can effectively improve electron transfer rate (Zhu et al., 2010).

To demonstrate the sensing application of GP, we first constructed a sensor by deposition of the aqueous dispersion of GP on a GCE surface. Fig. 5a shows CVs of a bare GCE, and GP/GCE in 0.2 M PBS at pH 7.4 in the presence of O_2 or N_2. It is seen that no obvious reduction peak is observed at both bare GCE and GP/GCE in the presence of N_2. In contrast, it is seen that bare GCE and GP/GCE

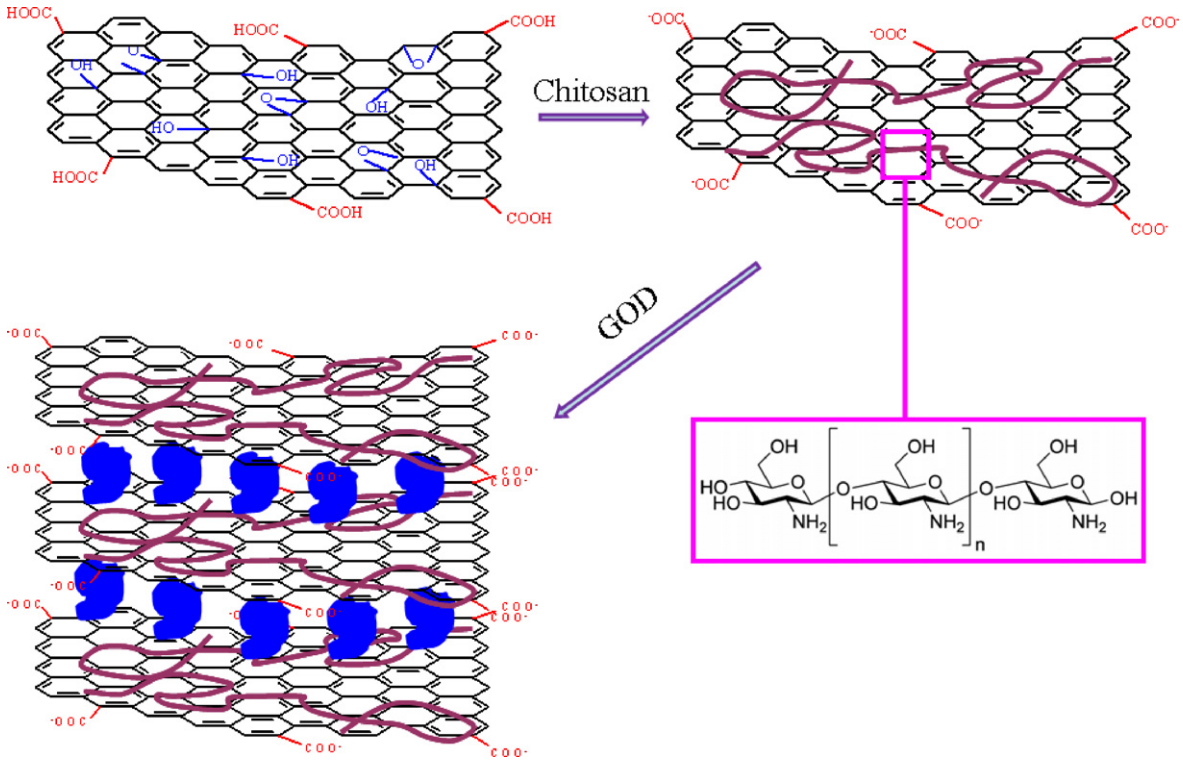

Fig. 4. A schmeme (not to scale) to illustrate the formation of GP from GO with the use of CS as a reducing and stabilizing agent and the subsequent preparation of GP–GOD nanostructures.

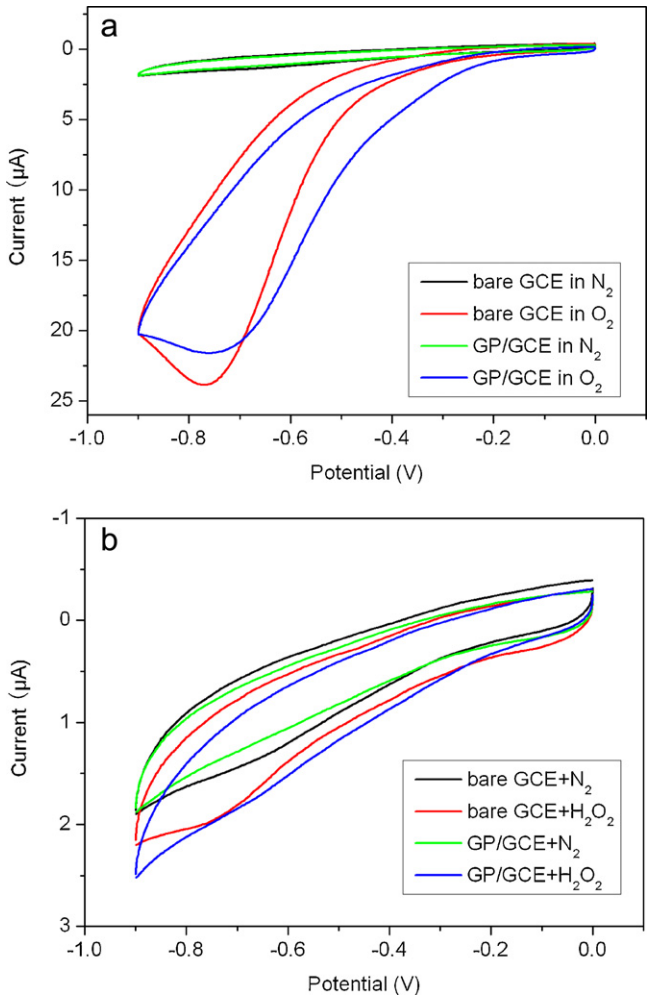

Fig. 5. (a) Cyclic voltammetries (CVs) of a bare GCE, and GP/GCE in 0.2 M PBS at pH 7.4 at various conditions (scan rate: 0.02 V/s). (b) CVs of a bare GCE, and GP/GCE in N_2 saturated 0.2 M PBS at pH 7.4 in the absence and presence of 1 mM H_2O_2.

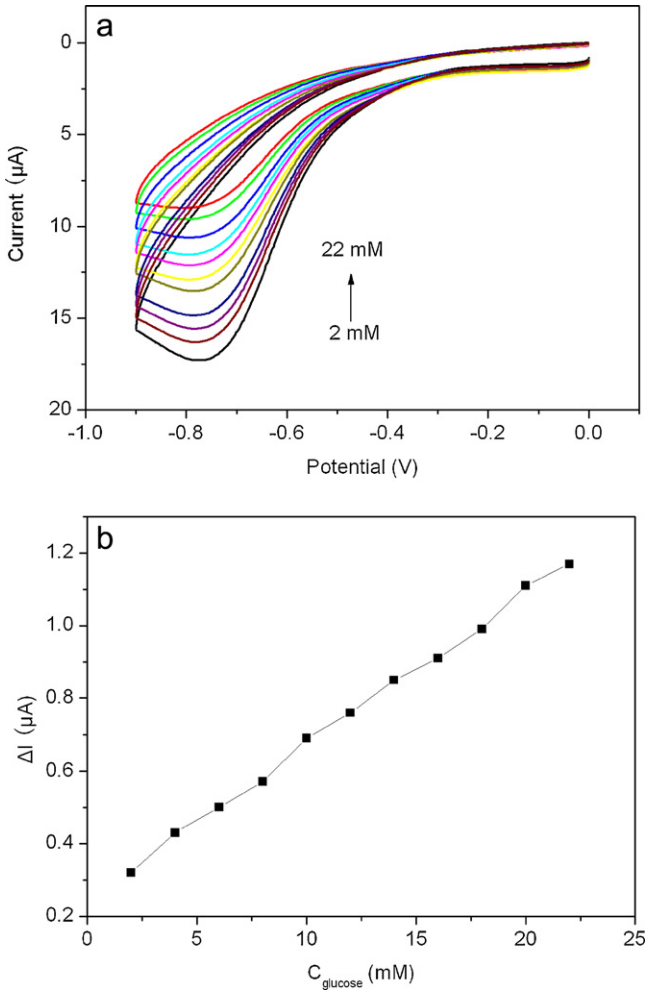

Fig. 6. (a) CVs of GP–GOD nanostructures modified electrode in O_2 saturated 0.2 M PBS at pH 7.4 in various concentrations of glucose. (b) The calibration curve corresponding to amperometric responses at −0.79 V.

exhibit a remarkable catalytic current peak about 24 μA in intensity at −0.77 V and about 22 μA in intensity at −0.75 V, respectively, in the presence of O_2, indicating good electrocatalysis toward O_2 reduction. As shown in Fig. 5b, it is also found that the response of both the bare GCE and the GP/GCE toward the reduction of H_2O_2 is pretty weak, revealing they exhibit relatively weak catalytic activity toward H_2O_2 reduction (Fig. 5b). All the above observations indicate the GP exhibits good catalytic activity toward O_2 reduction but poor catalytic activity toward H_2O_2 reduction.

On the base of the high electrocatalytic activity of GP toward O_2 reduction, a glucose sensor was further developed by deposition of GP–GOD nanostructures on GCE surface. Fig. 6a shows the CVs of GP–GOD modified electrode in 0.2 M PBS solution with various concentrations of glucose in saturated O_2. It is clearly seen that a strong reduction current peak at −0.79 is observed, which is attributed to the electrochemical reduction of O_2 and H_2O_2 (Shan et al., 2009). It is also found that the reduction current peaks became smaller and smaller with increasing the amount of glucose due to the consumption of O_2. Fig. 6b shows the calibration curve to corresponding amperometric responses at −0.79 V, revealing a linear relation against the concentration of glucose ranging from 2 to 22 mM (R = 0.9987). The detection limit is estimated to be 20 μM at a signal-to-noise ratio of 3. We also examined the electrocatalytic performance of GOD/GCE and GP/GCE toward glucose oxidation. It is seen that an increase of glucose in amount fails to lead to decrease reduction current at GP/GCE (Fig. S4), which can be attributed to the absence of GOD for glucose oxidation (Kang et al., 2009). Similarly, it is also found that increased amount of glucose does not give decreased reduction current at GOD/GCE (Fig. S5), which is due to the absence of graphene for improving electrons transfer (Shan et al., 2009). All these observations suggest that GP–GOD nanostructures exhibit excellent performance for detection of glucose due to the presence of active GOD and GP for improving electrons transfer. A comparison of the performance of our newly designed sensor with those already reported results regarding the performance of glucose detection is shown in Table S1, which indicates that our sensor exhibits relative lower detection limit and larger linear range than most of them.

4. Summary

We have developed a green and environment friendly route for preparation of well-stable GP dispersion by one-pot chemical reduction of GO with the use of CS as a reducing and stabilizing agent. We have further constructed GP–GOD nanostructures by a self-assembly route through the electrostatic interactions between the positively charged CS-stabilized GP and negatively charged GOD. The detection of glucose in the electrode modified by GP–GOD has also been demonstrated and it is revealed that the GP–GOD contained therein exhibits notable catalytic performance for detection of glucose. Our present findings provide us a low-cost

approach to production of stable aqueous dispersions of GP and graphene–enzyme nanostructures on a large scale for applications.

Appendix A. Supplementary data

Supplementary data associated with this article can be found, in the online version, at doi:10.1016/j.bios.2011.05.008.

References

Allen, M.J., Tung, V.C., Kaner, R.B., 2010. Chem. Rev. 110, 132–145.
Choi, B.G., Park, H., Park, T.J., Yang, M.H., Kim, J.S., Jang, S., Heo, N.S., Lee, S., Kong, J., Hong, W.H., 2010. ACS Nano 4, 2910–2918.
Dikin, D.A., Stankovich, S., Zimney, E.J., Piner, R.D., Dommett, G.H.B., 2007. Nature 448, 457–460.
Fan, X., Peng, W., Li, Y., Li, X., Wang, S., Zhang, G., Zhang, F., 2008. Adv. Mater. 20, 4490–4493.
Fang, M., Long, J., Zhao, W., Wang, L., Chen, G., 2010. Langmuir 26, 16771–16774.
Geim, A.K., Novoselov, K.S., 2007. Nat. Mater. 6, 183–191.
Guo, Y., Guo, S., Ren, J., Zhai, Y., Dong, S., Wang, E., 2010. ACS Nano 4, 4001–4007.
Huang, H., Yuan, Q., Yang, X., 2004. Colloid Surf. B: Biointerface 39, 31–37.
Hummers Jr., W.S., Offeman, R., 1958. J. Am. Chem. Soc. 80, 1339–11339.
Kang, X., Wang, J., Wu, H., Aksay, I.A., Liu, J., Lin, Y., 2009. Biosens. Bioelectron. 25, 901–905.
Li, D., Müller, M.B., Gilje, S., Kaner, R.B., Wallace, G.G., 2008. Nat. Nanotechnol. 3, 101–105.
Li, X., Wang, H., Robinson, J.T., Sanchez, H., Diankov, G., Dai, H., 2009. J. Am. Chem. Soc. 131, 15939–15944.
Liu, K., Zhang, J., Yang, G., Wang, C., Zhu, J., 2010a. Electrochem. Commun. 12, 402–405.
Liu, S., Tian, J., Wang, L., Li, H., Zhang, Y., Sun, X., 2010b. Macromolecules 43, 10078–10083.
Liu, Y., Yu, D., Zeng, C., Miao, Z., Dai, L., 2010c. Langmuir 26, 6158–6160.
Lu, J., Do, I., Drzal, L.T., Worden, R.M., Lee, I., 2008. ACS Nano 2, 1825–1832.
Lu, Q., Dong, X., Li, L., Hu, X., 2010. Talanta 82, 1344–1348.
Nethravathi, C., Rajamathi, M., 2008. Carbon 46, 1994–1998.
Novoselov, K.S., Geim, S.V., Morozov, S.V., Jiang, D., Zhang, Y., Dubonos, S.V., Grigorieva, I.V., Firsov, A.A., 2004. Science 306, 666–669.
Park, S., An, J., Piner, R.D., Jung, I., Yang, D., Velamakanni, A., Nguyen, S.T., Ruoff, R.S., 2008. Chem. Mater. 20, 6592–6594.
Patil, A.J., Vickery, J.L., Scott, T.B., Mann, S., 2009. Adv. Mater. 21, 3159–3164.
Pham, V.H., Cuong, T.V., Nguyen-Phan, T.D., Pham, H.D., Kim, E.J., Hur, S.H., Shin, E.N., Kim, S., Chung, J.S., 2010. Chem. Commun. 46, 4375–4377.
Potara, M., Maniu, D., Astilean, S., 2009. Nanotechnology 20, 315602.
Pumera, M., Ambrosi, A., Bonanni, A., Chng, E.L.K., Poh, H.L., 2010. Trac-Trends Anal. Chem. 29, 954–965.
Rao, C.N.R., Sood, A.K., Subrahmanyam, K.S., Govindaraj, A., 2009. Angew. Chem. Int. Ed. 48, 7752–7777.
Shan, C., Yang, H., Han, D., Zhang, Q., Ivaska, A., Niu, L., 2010. Biosens. Bioelectron. 25, 1070–1074.
Shan, C., Yang, H., Song, J., Han, D., Ivaska, A., Niu, L., 2009. Anal. Chem. 81, 2378–2382.
Shao, Y., Wang, J., Wu, H., Liu, J., Aksay, I.A., Lin, Y., 2010. Electroanalysis 22, 1027–1036.
Stankovich, S., Dikin, D.A., Dommett, G.H.B., Kohlhaas, K.M., Zimney, E.J., Stach, E.A., Piner, R.D., Nguyen, S.T., Ruoff, R.S., 2006. Nature 442, 282–286.
Wang, L., Zhang, X., Xiong, H., Wang, S., 2010a. Biosens. Bioelectron. 26, 991–995.
Wang, X., Bai, H., Liu, A., Shi, G., 2010b. J. Mater. Chem. 20, 9032–9036.
Wang, X., Li, X., Zhang, L., Yoon, Y., Weber, P.K., Wang, H., Guo, J., Dai, H., 2009a. Science 324, 768–771.
Wang, Z., Zhou, X., Zhang, J., Boey, F., Zhang, H., 2009b. J. Phys. Chem. C 113, 14071–14075.
Wei, D., Sun, W., Qian, W., Ye, Y., Ma, X., 2009. Carbohydr. Res. 344, 2375–2382.
Wu, H., Wang, J., Kang, X., Wang, C., Wang, D., Liu, J., Aksay, I.A., Lin, Y., 2009. Talanta 80, 403–406.
Wu, J., Xu, M., Zhao, G., 2010. Electrochem. Commun. 12, 175–177.
Xu, H., Dai, H., Chen, G., 2010. Talanta 81, 334–338.
Yang, M.H., Choi, B.G., Park, H., Hong, W.H., Lee, S.Y., Park, T.J., 2010a. Electroanalysis 22, 1223–1228.
Yang, X., Tu, Y., Li, L., Shang, S., Tao, X., 2010b. ACS Appl. Mater. Inter. 2, 1707–1713.
Yoo, E., Kim, J., Hosono, E., Zhou, H.S., Kudo, T., Homa, I., 2008. Nano Lett. 8, 2277–2282.
Zeng, G., Xing, Y., Gao, J., Wang, Z., Zhang, X., 2010a. Langmuir 26, 15022–15026.
Zeng, Q., Cheng, J., Tang, L., Liu, X., Liu, Y., Li, J., Jiang, J., 2010b. Adv. Funct. Mater. 20, 3366–3372.
Zhang, J., Yang, H., Shen, G., Cheng, P., Zhang, J., Guo, S., 2010. Chem. Commun. 46, 1112–1114.
Zhang, Y., Tan, Y.W., Stormer, H.L., Kim, P., 2005. Nature 438, 201–204.
Zhou, K., Zhu, Y., Yang, X., Li, C., 2010a. Electroanalysis 22, 259–264.
Zhou, K., Zhu, Y., Yang, X., Luo, L., Li, C., Luan, S., 2010b. Electrochim. Acta 55, 3055–3060.
Zhou, M., Zhai, Y., Dong, S., 2009a. Anal. Chem. 81, 5603–5613.
Zhou, Y., Bao, Q., Tang, L.A.L., Zhong, Y., Loh, K.P., 2009b. Chem. Mater. 21, 2950–2996.
Zhou, Y., Liu, S., Jiang, H., Yang, H., Chen, H., 2010c. Eletroanalysis 22, 1323–1328.
Zhu, C., Guo, S., Fang, Y., Dong, S., 2010. ACS Nano 4, 2429–2437.